Thermal Stability of Trifunctional Epoxy Resins Modified with Nanosized Calcium Carbonate

Fan-Long Jin† and Soo-Jin Park*

*Department of Chemistry, Inha University, Incheon 402-751, Korea. *E-mail: sjpark@inha.ac.kr*
†School of Chemical and Materials Engineering, Jilin Institute of Chemical Technology, Jilin 132022, P.R. China
Received July 29, 2008, Accepted December 18, 2008

Trifunctional epoxy resin triglycidyl paraaminophenol (TGPAP)/$CaCO_3$ nanocomposites were prepared using the melt blending method. The effects of nano-$CaCO_3$ content on the thermal behaviors, such as cure behavior, glass transition temperature (T_g), thermal stability, and the coefficient of thermal extension (CTE), were investigated by several techniques. Differential scanning calorimetry (DSC) results indicated that the cure reaction of the TGPAP epoxy resin was accelerated with the addition of nano-$CaCO_3$. When the nano-$CaCO_3$ content was increased, the T_g of the TGPAP/$CaCO_3$ nanocomposites did not obviously change, whereas the crosslinking density was linearly increased. The nanocomposites showed a higher thermal stability than that of the neat epoxy resin. This result could be attributed to the increased surface contact area between the nano-$CaCO_3$ particles and the epoxy matrix, as well as the high crosslinking density in the TGPAP/$CaCO_3$ nanocomposites. The CTE of the nanocomposites in the rubbery region was significantly decreased as the nano-$CaCO_3$ content was increased.

Key Words: Glass transition, Curing of polymers, Nanocomposites, Thermal properties, Crosslinking

Introduction

Epoxy resins are widely used as electrical and electronic adhesives and coatings, as well as in structural applications, because of their excellent mechanical and thermal properties.[1,2] However, diamines cured epoxy resins are brittle, which limits their many advanced applications. Therefore, several approaches have been made to improve the toughness of highly crosslinked epoxy resins.

Recently, polymer-inorganic nanocomposites, a new class of nanomaterial, have attracted considerable attention owing to their unique properties. Various fillers, such as nano-SiO_2, nano-$CaCO_3$, nano-ZnO, nano-Al_2O_3, and montmorillonite, have been added to polymers in order to improve the thermal and mechanical properties.[3-7] Among them, nano-$CaCO_3$, in the form of inorganic chalk, whiting and limestone particles, is the cheapest commercially available. Nano-$CaCO_3$ also has a low aspect ratio and a large surface area.[8] The low aspect ratio and large surface area of nano-$CaCO_3$ could result in strong interfacial interactions between the fillers and polymer matrix. Generally, the surface of nano-$CaCO_3$ particles is treated with organic compounds, such as stearic acid, to facilitate dispersion in the polymer matrix.[9]

$CaCO_3$-based polymer nanocomposites, such as EPDM/$CaCO_3$, poly(vinyl chloride)/$CaCO_3$, epoxy resins/$CaCO_3$, polypropylene/$CaCO_3$, HDPE/$CaCO_3$, and styrene-butadiene rubber/$CaCO_3$, are produced by incorporating nano-$CaCO_3$ into the polymer matrix.[4,8,10-13] Few studies on the preparation and mechanical properties of epoxy resins/$CaCO_3$ nanocomposites have been reported. Chen *et al*. reported the effect of $CaCO_3$ content on the mechanical properties of blocked polyurethane/epoxy interpenetrating polymer networks and they found the tensile strength, flexural strength, tensile modulus, and flexural modulus of IPNs increased with $CaCO_3$ content to a maximum value at 5, 10, 20, and 25 phr, respectively.[14] Wang *et al*. prepared epoxy resin/$CaCO_3$ nanocomposites by the methods of extruding, solusion, blending, as well as *in situ* and inclusion polymerization.[10] They found the resultant nanocomposite showed a 12 °C increase in T_g compared to the nanocomposite prepared by solution-blending and the tensile strain of nanocomposites rises as the nano-$CaCO_3$ content increases. They also introduced a mechanism by which the toughness of nanocomposites can be improved.[15]

In the present study, nanometer-$CaCO_3$-modified trifunctional epoxy resin triglycidyl paraaminophenol (TGPAP), nanocomposites were prepared using the melt blending method. The effects of the nano-$CaCO_3$ contents on the curing behaviors, dynamic mechanical properties, thermal stabilities, and thermal mechanical properties of the TGPAP/$CaCO_3$ nanocomposites were studied by differential scanning calorimetry (DSC), dynamic mechanical analysis (DMA), thermogravimetric analysis (TGA), and thermal mechanical analysis (TMA).

Experimental

Materials. TGPAP of an epoxide equivalent weight of 110-115 g/eq was kindly provided as an epoxy matrix by Kukdo Chem. of Korea (XDT-3300). Nano-$CaCO_3$ of a mean particle size of 40-70 nm and a specific surface of 20-30 m^2/g, used in this study, was supplied by WINNOFIL'S, Solvay. The content of the stearic acid on the nano-$CaCO_3$ surfaces, determined by TGA, was 3.5 wt%.[16] The curing agent was 4,4'-diamonodiphenyl methane (DDM), purchased from Aldrich. The chemical structures of TGPAP and DDM are shown in Figure 1.

Sample preparation. The nano-$CaCO_3$ content was varied from 2 to 8 wt%. TGPAP was heated in an oil bath at 80 °C for 30 min, and then, the determined amount of nano-$CaCO_3$ was added to the resin. The mixtures were mixed with a magnetic

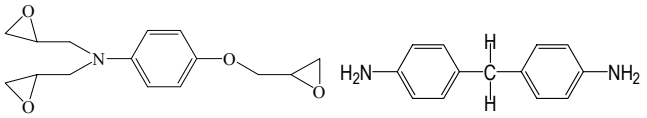

Triglycidyl paraaminophenol (TGPAP) 4,4'-Diaminodiphenyl methane (DDM)

Figure 1. Chemical structures of the materials used.

stirrer for 1 h, and then sonicated using sonicator. The mixture was degassed in a vacuum oven, and then an equivalent weight of DDM was added to the mixture. The preparation of the specimens for thermal tests was as follows: bubble-free mixtures were poured into the mold and typical curing was carried out at 110 °C for 1 h (primary curing), at 150 °C for 2 h (secondary curing), and at 180 °C for 1 h (post-curing) in a convection oven. The specimens were cut to suitable dimensions for the thermal tests.

Characterization and measurements. The cure behaviors of nano-$CaCO_3$-modified epoxy resin were studied using a differential scanning calorimeter (Perkin Elmer, DSC6) at a heating rate of 10 °C/min under a nitrogen flow of 30 ml/min.

The dynamic mechanical properties were determined with a dynamic mechanical analyzer (RDS-II, Rhemetrics Co.) at a frequency of 1 Hz, a 30 to 300 °C temperature range, and a scan rate of 5 °C/min. The sample size was 3×12×60 mm^3. The crosslinking density (ρ) of the cured specimens was calculated from the equilibrium storage modulus in the rubber region over the α-relaxation temperature according to the rubber elasticity theory.[17] That is,

$$\rho = M_C G' / \phi RT \quad (1)$$

where T_g is the glass transition temperature (K), G' the modulus of epoxy nanocomposites (GPa), ø the front factor close to 1 according to Murayama and Bell,[18] R the gas constant [8.3146 J/(mol K)], and T the absolute temperature at T_g + 30 °C (K).

Fourier-transform infrared spectra were determined with a Bio-Rad digilab FTS-165 spectrometer using KBr pellets. The peak at 910 cm^{-1} indicates the epoxide groups and was used to monitor their consumption in this study. The aromatic C=C stretching vibration at 1513 cm^{-1} was chosen reference peak. The conversion of cure reaction was calculated from the initial area of the epoxide groups and their corresponding value at different nano-$CaCO_3$ contents according to the following equation:[19,20]

$$Conversion = \left(1 - \frac{(A_{peak})_{cure}(A_{ref})_{uncure}}{(A_{ref})_{cure}(A_{peak})_{uncure}}\right) \times 100 \quad (2)$$

where $(A_{peak})_{uncure}$ and $(A_{peak})_{cure}$ are the area of the active epoxide groups before and after cure, and $(A_{ref})_{uncure}$ and $(A_{ref})_{uncure}$ the area of the reference peaks before and after cure.

The thermal stability of the cured samples was investigated with a du Pont TGA-2950 analyzer from 30 to 850 °C at a heating rate of 10 °C/min in a nitrogen atmosphere. The decomposition activation energy was calculated from TGA curves using the integral method of Coats and Redfern's equation, as follows:[21]

$$\ln\frac{\alpha}{T^2} = \ln\frac{AR}{\beta E_d}\left(\frac{1-2RT}{E_d}\right) - \frac{E_d}{RT} \quad (3)$$

where α is the decomposed fraction, T the degradation temperature (K), A the preexponential factor, β the heating rate (K/min), E_d the decomposition activation energy (kJ/mol), and R the gas constant [8.3146 J/(mol K)].

The coefficient of thermal expansion (CTE) was obtained by thermal mechanical analysis (RDS-II, Rhemetrics Co.) at a heating rate of 5 °C/min under a nitrogen atmosphere.

Results and Discussion

Cure behaviors. The cure behaviors of TGPAP epoxy resin modified with nanometer calcium carbonate (nano-$CaCO_3$) were investigated using DSC. The temperature-ranging DSC scans for the neat epoxy resin and the nano-$CaCO_3$-modified epoxy resin are shown in Figure 2. All of the DSC thermograms exhibit a single peak, and the peak temperature of the epoxy resin is shifted to low temperature with the addition of nano-$CaCO_3$. It is well known that primary and secondary amines react by nucleophilic addition to epoxide. And proton donors, such as acids, phenols, alcohol, and toluene, act as catalysts and accelerate the epoxide-amine ring-opening. Scheme 1 shows the mechanism of acceleration. Upon addition of nano-$CaCO_3$ to the epoxide-amine system, a hydrogen bond was formed between the oxygen of the epoxide and the hydrogen of searic acid on the nano-$CaCO_3$ surfaces, which resulted in the acceleration of the amine-epoxide reaction via a termolecular hydrogen-bonded transition stage.[22]

Dynamic mechanical properties. The dynamic mechanical properties were measured by DMA. The tan δ over a certain range of temperature for the TGPAP/$CaCO_3$ nanocomposites at various nano-$CaCO_3$ contents is shown in Figure 3. The glass transition temperature (T_g) was determined as a maxi-

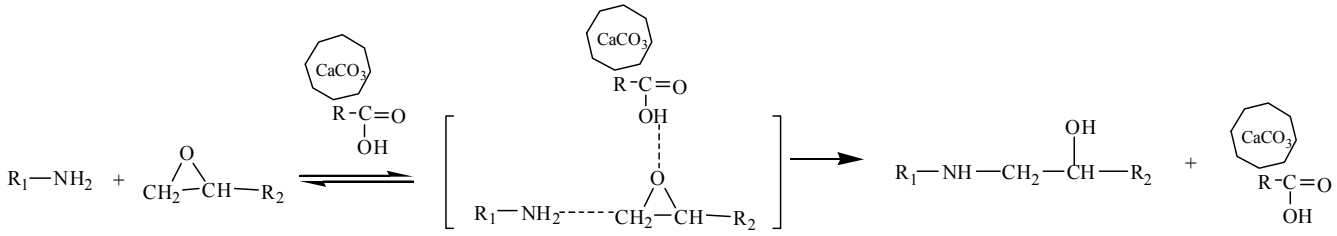

Scheme 1. Cure mechanism of epoxide and amine accelerated by proton donors.

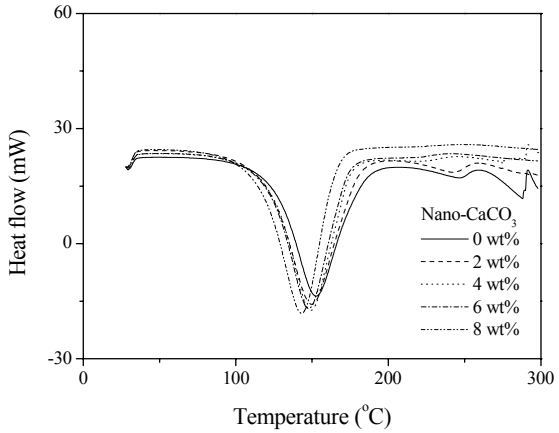

Figure 2. DSC runs in the temperature range between 30 and 300 °C for nano-$CaCO_3$-modified TGPAP epoxy resin (heating rate of 10 °C/min).

Table 1. DMA results for TGPAP/$CaCO_3$ nanocomposites

Nano-$CaCO_3$ content (wt%)	T_g (°C)	G' (MPa)	ρ (g/cm)
0	240	25.4	1.502
2	238	26.1	1.518
4	240	27.4	1.556
6	239	28.5	1.587
8	232	29.7	1.643

mum value of tan δ occurs. The T_g determined from the DMA curves is listed in Table 1. The T_g of the nanocomposites was not significantly varied with nano-$CaCO_3$ content up to 6 wt%. When nano-$CaCO_3$ content is 8 wt%, T_g was decreased from 240 °C for the neat epoxy resin to 232 °C for the nanocomposites, which due to the uncompleted dispersion at high nano-$CaCO_3$ content. Li *et al*. observed a similar phenomenon in rigid polystyrene/$CaCO_3$ nanocomposites.[23]

The crosslinking density (ρ) of the TGPAP/$CaCO_3$ nanocomposites was calculated from the DMA data on the basis of equation 1. The results are summarized in Table 1. The ρ value was slightly increased by increasing the nano-$CaCO_3$ content. This result can be explained according to the conversion of the cure reaction.

The IR spectra of the TGPAP epoxy resin before and after

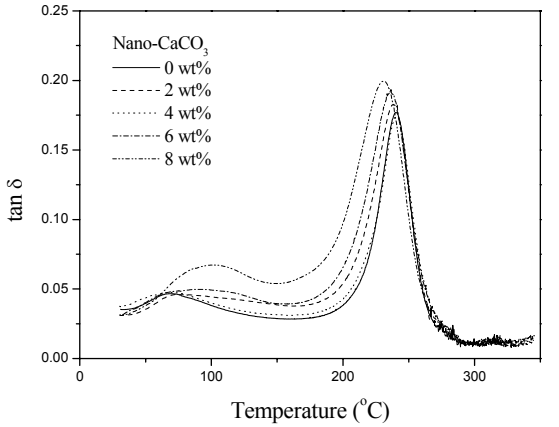

Figure 3. tan ρ as a function of temperature for TGPAP/DDM and TGPAP/$CaCO_3$ nanocomposites.

Table 2. Conversion of TGPAP/$CaCO_3$ nanocomposites calculated from FT-IR spectra

Nano-$CaCO_3$ content (wt%)	0	2	4	6	8
Conversion (%)	84.7	86.9	88.1	89.2	91.4

Table 3. Thermal stability factors for TGPAP/$CaCO_3$ nanocomposites

Nano-$CaCO_3$ content (wt%)	IDT (°C)	T_{max} (°C)	E_d (kJ/mol)	Char (%)[a]
0	279	354	57	18.9
2	299	370	67	22.0
4	300	373	68	21.1
6	302	377	69	23.7
8	309	381	71	27.5

[a]Char at 850 °C

curing are shown in Figure 4. The peak at 910 cm^{-1} indicates the epoxide groups and was used to monitor their consumption. The conversion of the cure reaction for the neat epoxy resin and the nanocomposites was calculated from the IR spectra based on equation 2, and the results are presented in Table 2. The conversion varied from 84.7 to 88.1% for 4 wt% nano-$CaCO_3$ and from 84.7 to 91.4% for 8 wt% nano-$CaCO_3$. The stearic acid on the $CaCO_3$ surfaces accelerated the amine-

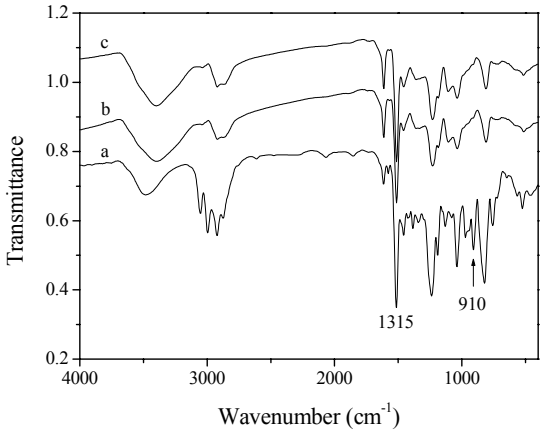

Figure 4. FT-IR spectra of neat TGPAP epoxy resin (a), TGPAP/DDM (b), and TGPAP/$CaCO_3$ nanocomposites (c).

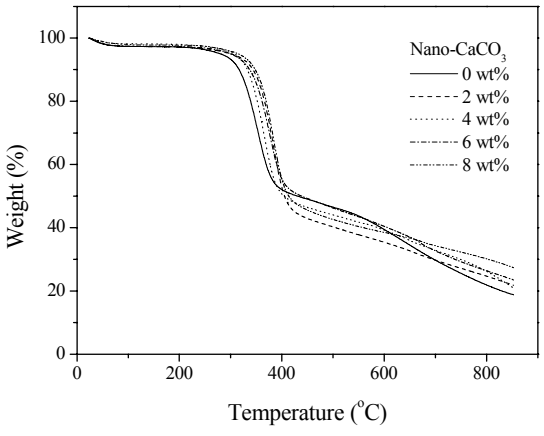

Figure 5. TGA thermograms of TGPAP/$CaCO_3$ nanocomposites as a function of nano-$CaCO_3$ content.

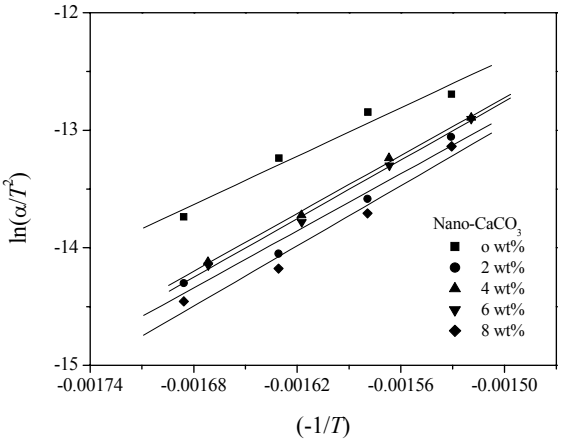

Figure 6. Plots of ln(a/T^2) *versus* (-1/T) for TGPAP/$CaCO_3$ nanocomposites.

epoxide reaction via a termolecular hydrogen-bonded transition stage, thus increasing the epoxide conversion, and increasing, in turn, the crosslinking density in the TGPAP/$CaCO_3$ nanocomposites.[22]

Thermal stability. The thermal stabilities of the TGPAP/$CaCO_3$ nanocomposites were studied by means of TGA. The TGA thermograms for the neat epoxy resin and TGPAP/$CaCO_3$ nanocomposites are shown in Figure 5. The thermal stability factors, including the initial decomposing temperature (IDT), the temperature at the maximum rate of weight loss (T_{max}), and the decomposition activation energy (E_d), were calculated from the TGA thermograms.[24,25] The E_d value was calculated from ln(a/T^2) *versus* (-1/T) plots on the basis of equation 3, as shown in Figure 6.

The thermal stability factors for the TGPAP/$CaCO_3$ nanocomposites are summarized in Table 3. The thermal stability of the nanocomposites was significantly enhanced by the addition of nano-$CaCO_3$. In the neat epoxy system, the degradation started at around 280 °C. When nano-$CaCO_3$ was added to the epoxy matrix, the IDT of the nanocomposites was at least 20 °C higher than that of the neat epoxy system. The T_{max} of the neat epoxy system was 354 °C, whereas upon addition of nano-$CaCO_3$ to the epoxy matrix, the T_{max} of the nanocomposites appeared within the range of 370-384 °C. Meanwhile, the E_d of the neat epoxy system was 57 kJ/mol, and the E_d of the nanocomposites was about 10 kJ/mol higher than that of the neat epoxy system. These results can be interpreted with reference to the addition of nano-$CaCO_3$ to the epoxy matrix, which increased the surface contact area between the nano-$CaCO_3$ particles and the epoxy matrix, which in turn prevented the heat diffusion during decomposition of the TGPAP/$CaCO_3$ nanocomposites.[8,16] The results can be attributed also to the increased cosslinking density of the nanocomposites. The char content for the nanocomposites at 850 °C also was increased with the addition of nano-$CaCO_3$. A similar observation was reported by Chen *et al*. using rigid poly(vinyl chloride)/calcium carbonate nanocomposites.[8]

Thermal mechanical properties. The dimension changes of the TGPAP/$CaCO_3$ nanocomposites were measured by TMA in the temperature range from 30 to 300 °C. The CTE was determined from the TMA curves, and the results are listed in Table 4. When the nano-$CaCO_3$ content was increased, the CTE of the nanocomposites in the glassy region did not significantly vary. This result is in agreement with the glass transition temperature obtained by DMA. The CTE of the nanocomposites in the rubbery region was significantly decreased as the nano-$CaCO_3$ content was increased. This result can be caused by dispersion of nano-$CaCO_3$ into the epoxy matrix, thus increasing an intermolecular interaction, such as hydrogen bonding, between the hydroxyl group in the epoxy network and the hydroxyl group of stearic acid on the $CaCO_3$ surfaces, resulting in the prohibition of molecular chain movement in TGPAP/$CaCO_3$ nanocomposites.[16,26]

Table 4. Thermal mechanical analysis of TGPAP/$CaCO_3$ nanocomposites

Nano-$CaCO_3$ content (wt%)	CTE (10^{-5} °C)	
	Glassy region	Rubbery region
0	70	408
2	67	347
4	67	318
6	69	311
8	70	264

Conclusions

The cure behaviors, crosslinking density, thermal stabilities, and coefficient of thermal expansion (CTE) of TGPAP/$CaCO_3$ nanocomposites were investigated using several techniques. As one experimental result, the peak temperature of the nano-$CaCO_3$-modified TGPAP epoxy resin was shifted to a lower temperature by increasing the nano-$CaCO_3$ content, which, due to the amine-epoxide reaction, was accelerated by the addition of nano-$CaCO_3$. The crosslinking density of the TGPAP/$CaCO_3$ nanocomposites was linearly increased as the nano-$CaCO_3$ content was increased. The nanocomposites showed a higher thermal stability than that of the neat epoxy resins. This could be attributed to the addition of nano-$CaCO_3$ into the epoxy matrix, thus increasing the surface contact area between the nano-$CaCO_3$ particles and the epoxy matrix, leading in turn to an increase in the absorption of heat energy during decomposition of the TGPAP/$CaCO_3$ nanocomposites. When the nano-$CaCO_3$ content was increased, the CTE of the nanocomposites in the glassy region was not obviously changed, whereas the CTE in the rubbery region was significantly increased.

References

1. Bauer, R. S. *Epoxy Resin Chemistry*, Advanced in Chemistry Series, No 114; American Chemical Society: Washington DC, 1979; p 1.
2. Gowda, S. K. N.; Mahendra, K. N. *Bull. Korean Chem. Soc.* **2006**, *27*, 1542.
3. Rong, M. Z.; Zhang, M. Q.; Zheng, Y. X.; Zeng, H. M.; Friedrich, K. *Polymer* **2001**, *42*, 3301.
4. Zhou, Y.; Wang, S.; Zhang, Y.; Zhang, Y. *J. Polym. Sci. Part B: Polym. Phys.* **2006**, *44*, 1226.
5. Zhang, Z. Z.; Su, F. H.; Wang, K.; Jiang, W.; Men, X. H.; Liu, W. M. *Mater. Sci. Eng. A* **2005**, *404*, 251.

6. Naous, W.; Yu, X. Y.; Zhang, Q. X.; Naito, K.; Kagawa, Y. *J. Polym. Sci. Part B: Polym. Phys.* **2006**, *44*, 1466.
7. Jin, F. L.; Rhee, K. Y.; Park, S. J. *Mater. Sci. Eng. A* **2006**, *435-436*, 429.
8. Chen, C. H.; Teng, C. C.; Su, S. F.; Wu, W. C.; Yang, C. H. *J. Polym. Sci. Part B: Polym. Phys.* **2006**, *44*, 451.
9. Li, G.; Mai, K. C.; Feng, K. C.; Huang, Y. P. *Polym. Int.* **2006**, *55*, 891.
10. Shi, Q.; Wang, L.; Yu, H.; Jiang, S.; Zhao, Z.; Dong, X. *Macromol. Mater. Eng.* **2006**, *291*, 53.
11. Zhang, L.; Li, C.; Huang, R. *J. Polym. Sci. Part B: Polym. Phys.* **2004**, *42*, 1656.
12. Wang, Y.; Lu, J.; Wang, G. *J. Appl. Polym. Sci.* **1997**, *64*, 1275.
13. Mishra, S.; Shimpi, N. G. *J. Appl. Polym. Sci.* **2005**, *98*, 2563.
14. Chen, C. H.; Sun, Y. Y. *J. Appl. Polym. Sci.* **2006**, *99*, 1826.
15. Yu, H.; Wang, L.; Shi, Q.; Jiang, S.; Jiang, G. *J. Appl. Polym. Sci.* **2006**, *101*, 2656.
16. Jin, F. L.; Park, S. J. *Mater. Sci. Eng. A* **2008**, *475*, 190.
17. Plangsangmas, L.; Mecholsky, J. J.; Brennan, A. B. *J. Appl. Polym. Sci.* **1999**, *72*, 257.
18. Murayama, T.; Bell, J. P. *J. Polym. Sci. Part A-2* **1970**, *8*, 437.
19. Park, S. J.; Jin, F. L. *Polym. Int.* **2005**, *54*, 705.
20. Rath, S. K.; Boey, F. Y. C.; Abadie, M. J. M. *Polym. Int.* **2004**, *53*, 857.
21. Coats, A. W.; Redferm, J. W. *J. Polym. Sci. Polym. Lett.* **1965**, *3*, 917.
22. May, C. A. *Epoxy Resins, Chemistry and Technology*; Marcel Dekker: New York, 1988; p 298.
23. Li, G.; Mai, K.; Feng, K. *J. Appl. Polym. Sci.* **2006**, *99*, 2138.
24. Jin, F. L.; Park, S. J. *J. Polym. Sci. Part B: Polym. Phys.* **2006**, *44*, 3348.
25. Jin, F. L.; Park, S. J. *Polym. Degrad. Stab.* **2007**, *92*, 509.
26. Park, S. J.; Jin, F. L.; Lee, C. *Mater. Sci. Eng. A* **2005**, *402*, 335.